Biomass Conversion and Biorefinery (2022) 12:2715–2726
https://doi.org/10.1007/s13399-020-00828-5

ORIGINAL ARTICLE

Zinc chloride–activated glycerine pitch distillate for methylene blue removal—isotherm, kinetics and thermodynamics

Pua Eng Hock[1,2] · Muhammad Abbas Ahmad Zaini[1,2]

Received: 14 March 2020 / Revised: 28 May 2020 / Accepted: 19 June 2020 / Published online: 27 June 2020
© Springer-Verlag GmbH Germany, part of Springer Nature 2020

Abstract

This work was aimed at evaluating the adsorptive properties of glycerine pitch distillate-based activated carbons by zinc chloride activation. A commercial activated carbon derived from petroleum pitch distillate was employed for comparison. Activated carbons were characterized for elemental composition, textural characteristics, and surface chemistry. The adsorption data were analyzed using isotherm and kinetic models, and thermodynamic parameters. The specific surface area of activated carbons is between 50.4 and 804 m^2/g. The maximum methylene blue capacity of 368 mg/g is comparable with that of commercial activated carbon. The fitting of adsorption data suggests a monolayer coverage of dye molecules onto activated carbon via chemisorption where a cooperative mechanism of particle diffusion and film diffusion may be the controlling mechanism. The adsorption is spontaneous for potential applications in dye wastewater treatment.

Keywords Activated carbon · Adsorption · Zinc chloride activation · Glycerine pitch distillate · Methylene blue

1 Introduction

Activated carbon is a highly porous adsorptive medium that has a complex structure composed primarily of carbon atoms. It consists of pore networks with channels generated inside a rigid skeleton of disordered layers of graphitic structure, linked together by chemical bonds, stacked unevenly, hence generating nooks, crannies, cracks, and crevices between the carbon layers [1]. Activated carbon can be manufactured from several carbonaceous materials such as palm kernel shell [2], empty fruit bunch [3], and rubber seed shell [4] via chemical or physical activation.

Chemical activation has several advantages over physical activation because of lower activation temperature (~ 550 °C), high activated carbon yield, and high surface area for effective water pollutant removal [1]. Zinc chloride ($ZnCl_2$) is a commonly used dehydrating agent in chemical activation [5]. In $ZnCl_2$ activation, the liquid chemical is intercalated into the carbon matrix to produce pores at a temperature above its melting point [6]. The activation often turns the carbonaceous material into activated carbon with high surface area through pyrolysis at high temperature [7]. A large surface area aids in a higher performance of activated carbon [5]. The intrinsic pore network in the lattice structure enables the elimination of impurities from liquid media through a mechanism known as adsorption [1].

There is an increasing demand to synthesize low-cost activated carbon due to the escalating price of commercial activated carbon [1]. Glycerine pitch distillate (GPD) is a promising candidate for raw material of activated carbon. The semi-liquid residue from a palm oil refinery is a waste by-product of less commercial value which mainly consists of polyglycerols, glycerine from soap lye, inorganic salts, and salts of organic acids [8]. The material has been used as biodiesel feedstock and fuel in boiler, and in a fuel blend with diesel to reduce the emission in boiler [9]. To date, there is no dedicated research done to capitalize this resource towards a sustainable environment. The closest related materials found in literature are

Electronic supplementary material The online version of this article (https://doi.org/10.1007/s13399-020-00828-5) contains supplementary material, which is available to authorized users.

✉ Muhammad Abbas Ahmad Zaini
abbas@cheme.utm.my

[1] Centre of Lipids Engineering & Applied Research (CLEAR), Ibnu-Sina Institute for Scientific & Industrial Research, Universiti Teknologi Malaysia, 81310 Johor Bahru, Johor, Malaysia

[2] School of Chemical & Energy Engineering, Faculty of Engineering, Universiti Teknologi Malaysia, 81310 Johor Bahru, Johor, Malaysia

biodiesel waste [10] and palm fatty acid distillate [11]. Therefore, the present work is aimed to evaluate the conversion of GPD into activated carbons and their performance in methylene blue dye removal. The activated carbons were characterized, and the adsorption data were analyzed using equilibrium and kinetic models, and thermodynamic parameters to shed insight into adsorption mechanisms. The outcome of this work shall enrich the body of knowledge in the field of environmental engineering, particularly in activated carbon synthesis and adsorption.

2 Materials and methods

2.1 Materials

Glycerine pitch distillate was supplied by oil palm refinery in the Johor state of Malaysia. Zinc chloride, hydrochloric acid (30%), and methylene blue were purchased from R&M Chemicals (Essex, UK). Figure S1 shows the molecular structure of methylene blue [12]. Sodium hydroxide (96%) was supplied by Bendosen (Johor, Malaysia). All chemical reagents are of analytical reagent grade and were used as received without further treatment.

2.2 Preparation and characterization of activated carbon

Activated carbons were prepared from GPD by chemical activation using $ZnCl_2$. Ten grams of GPD was mixed with $ZnCl_2$ at weight ratios ($ZnCl_2$:GPD) of 0, 0.5, 1, 1.5, 2, 2.5, and 3. The mixture was stirred and heated at 90 °C for 10 min. Then, the mixture was added into a crucible, covered with aluminum foil to induce an anoxic environment by minimizing contact with air. After that, the crucible was placed inside a muffle furnace for activation at 500 °C for 30 min. The operating condition was recommended from several $ZnCl_2$ activation studies [5]. The resultant activated carbons were soaked in 0.1 M HCl overnight for partial demineralization and refluxed several times with hot distilled water to a constant pH. Table 1 summarizes the designation of activated carbons prepared by $ZnCl_2$ activation.

The thermal degradation profile was obtained using a thermogravimetric analyzer (TGA-50, Shimadzu, Japan), operating under N_2 flow at a heating rate of 10 °C/min. The elemental composition was determined using a Vario Micro Cube analyzer (Elementar, Germany). The surface composition and morphology were obtained by a SEM-EDX integrated machine (TM3000, Hitachi, Japan). The textural properties of activated carbon were determined at a liquid N_2 temperature of 77 K using a surface area analyzer (ASAP2020, Micromeritics, USA). The peaks of functional groups of activated carbon were recorded by an attenuated total reflectance FTIR spectrometer (Spectrum One, PerkinElmer, USA).

Table 1 Designation of activated carbons

Mass impregnation ratio (GPD:$ZnCl_2$)	Designation
1:0	R0
1:0.5	R0.5
1:1	R1
1:1.5	R1.5
1:2	R2
1:2.5	R2.5
1:3	R3

The pH point of zero charge (pH_{PZC}) describes the condition when the net electrical charge density on a surface is zero. Different batches of 0.1 M NaCl of varying solution pH values between 2 and 11 were prepared. The pH was adjusted by adding small drops of 0.1 M HCl and 0.1 M NaOH. Upon equilibrium, 50 mg of activated carbon was added into the solution, and the mixture was equilibrated at 30 °C for 24 h. After that, the final pH was measured using a pH meter (HI 8424, Hanna Instruments, UK). The final pH was plotted against the initial pH, and the pH_{PZC} was determined at the point where the initial pH is equal to the final pH.

For Boehm titration, batches of 15 mL solutions of $NaHCO_3$ (0.1 M), Na_2CO_3 (0.05 M), NaOH (0.1 M), and HCl (0.1 M) were prepared. 0.1 g of activated carbon was brought into contact with each solution at room temperature for 48 h. Then, 5-mL aliquots were back titrated with 0.05 M HCl and 0.1 M NaOH for acidic and basic groups, respectively. Neutralization points were observed using pH indicators, i.e., phenolphthalein solution for titration of strong base with strong acid and methyl red solution for titration of weak base with strong acid. The concentration of each functional group was calculated by the following assumptions: (i) $NaHCO_3$ neutralizes only carboxylic groups, (ii) Na_2CO_3 neutralizes carboxylic and lactonic groups, (iii) NaOH neutralizes carboxylic, lactonic, and phenolic groups, and (iv) HCl neutralizes basic groups.

2.3 Batch adsorption studies

Fifty milligrams of activated carbon was added into a flask containing 30 mL of methylene blue dye solution of varying concentrations. The mixture was equilibrated for 72 h. The operating conditions of contact time and temperature were also evaluated. The concentration of MB was analyzed using a UV-vis spectrophotometer (DU-8200, Drawell Scientific, China) at a wavelength of 665 nm.

The adsorption capacity at equilibrium, q_e (mg/g), was calculated as:

$$q_e = \frac{(C_o - C_e)V}{m} \quad (1)$$

where C_o and C_e (mg/L) are initial concentration and equilibrium concentration, respectively, V (L) is the solution volume, and m (g) is the mass of activated carbon.

Similar settings were repeated for adsorption kinetics. Fifty milligrams of activated carbon was added to flasks containing 30 mL of dye solution with different concentrations. The condition was fixed at ambient temperature and the concentration was measured at different time intervals. The adsorption capacity at time t, q_t (mg/g), was calculated as:

$$Q_t = \frac{(C_o - C_t)V}{m} \quad (2)$$

where C_t (mg/L) is the concentration at time, t.

The thermodynamic parameters were determined from the equilibrium adsorption of selected activated carbons at different concentrations and solution temperatures. For the effects of concentration, time, and temperature, the solution pH was left unadjusted for the entire adsorption process. All experiments and measurements were reproduced in duplicate and the average values were reported. The adsorption data were analyzed using adsorption models to describe the transport behavior and removal mechanisms. The isotherm and kinetic models and thermodynamic parameters are summarized in Table S1. The non-linear equations were solved using Microsoft Excel solver.

3 Results and discussion

3.1 Characteristics of activated carbon

Figure S2 shows the thermogravimetric profile of GPD. Glycerine pitch distillate is thermally unstable as it is easily vaporized as temperature increases. Nearly 50% of the weight is lost at 260 °C, and the weight has completely vanished as gasses at 980 °C. Generally, the weight loss profile can be divided into three distinct phases. The first phase ranging between room temperature and 178 °C is attributed to the liberation of moisture and light volatiles. This corresponds to a peak centered at 128 °C. The moisture content of GPD is estimated at 22%. The ignition temperature is presumed to be around 178 °C during which the combustion and decomposition of GPD are intensified, leading to a sharp weight loss at the second phase with a peak at 266 °C. The second phase is associated with the liberation of heavier fractions and the decomposition of molecular organic compounds. Next, the profile shows a gradual weight loss from 93.2 to 96.9% at the third phase, with burnout temperature of 980 °C. GPD consists of simple structure compounds that are readily broken down and easily degraded at high temperatures. At 980 °C, the remaining residue or ash content was recorded at 3.1%. The degradation of material as displayed by peaks at 500 °C could be due to the burning off of higher density carbon structures [13]. The third phase normally corresponds to the combustion of fixed carbon [14]. It may be deduced that the suitable carbonization temperature for GPD activation is 550 °C.

Table 2 shows the elemental composition of activated carbons derived from GPD, namely R1 and R2, and commercial petroleum pitch distillate activated carbon (PPD). The carbon content increased from 4.72 to 56.6% with increasing $ZnCl_2$ ratio from 1 to 2. A high $ZnCl_2$ concentration used in activation improves the carbon content of GPD activated carbon through the formation of aromatic graphitic structure [15]. The liberation of volatiles enhances the pore development, hence increasing the carbon content, pore volume, surface area, and porosity of activated carbon. Also, $ZnCl_2$ has been reported to inhibit the formation of tar, which can avert the pore development [5]. Conversely, an insufficient $ZnCl_2$ amount usually leads to an underdeveloped structure of carbon network.

The yield, methylene blue capacity, and surface area of activated carbons are summarized in Table 3. The surface area of activated carbons is in the range of 50.4 to 804 m^2/g. Activation at ratio 1 yields a 16.6% activated carbon (R1) with a surface area of 804 m^2/g. R1 demonstrates a comparable BET surface area with commercial PPD. The yield of activated carbon increases from 9.68% at ratio 0 (R0) and decreases to 9.4% at ratio 2.5 (R2.5). A high impregnation ratio permits more zinc ions to penetrate the carbon network, causing intensive dehydration or volatilization to excessively remove light and volatile matters through the collapse of aliphatic and aromatic bonds [16]. Consequently, the yield, surface area, and microporosity of activated carbon decreased with increasing impregnation ratio.

Figure S3 illustrates the N_2 adsorption-desorption profiles of activated carbons, and the respective textural properties are

Table 2 Elemental composition of activated carbons

Activated carbon	Element (dry-ash-free, wt%)				
	Carbon	Hydrogen	Nitrogen	Oxygen*	Sulfur
R1	4.72	1.43	0.109	93.7	0.352
R2	56.5	2.42	0.425	40.4	0.310
PPD	78.4	0.814	0.164	20.1	0.525

*Calculated by difference

Table 3 Yield, methylene blue capacity (Q_m), and surface area of activated carbons

Sample	Yield (%)	Methylene blue capacity, Q_m (mg/g)	Specific surface area, S_{BET} (m^2/g)
R0	9.68	68	50.4
R1	16.6	151	804
R2	15.5	368	377
R2.5	9.40	342	267
PPD	-	383	1187

summarized in Table S2. PPD demonstrates a type I isotherm according to the IUPAC classification, suggesting a monolayer formation of N_2 molecules onto microporous solid with a small external surface. R2 and R2.5 show a type IV isotherm with H3 hysteresis loop, indicating mesoporous solid with particle aggregates forming slit-like pores [17]. From Table S2, PPD is microporous (67% microporosity) with average pore width of 1.9 nm. The GPD activated carbons are highly mesoporous with pore widths of 2.9 nm and 4.1 nm for R2.5 and R2, respectively.

The effect of pore drilling has resulted in irregularly shaped pores. The adsorption of large dye molecules (e.g., methylene blue, size 0.59 nm × 1.4 nm) might be enhanced because of the presence of mesopores [18]. GPD activated carbons could be a promising adsorbent for dyes wastewater treatment.

Figure 1 shows the SEM images of R0, R2, and PPD. The surface of R2 is irregular and rough with holes and splits representing the entrances for pore channels. The pore networks give rise to a hierarchical structure in promoting interaction probabilities with adsorbate molecules for adsorption. R0 displays a needle-like surface because of the aggressive burning off of semi-solid GPD in the absence of an activating agent. In other words, it is evident that $ZnCl_2$ activation preserves the carbon yield.

Figure 2 shows the EDX mapping of activated carbons, and the surface composition is given in Table S3. R0 shows an

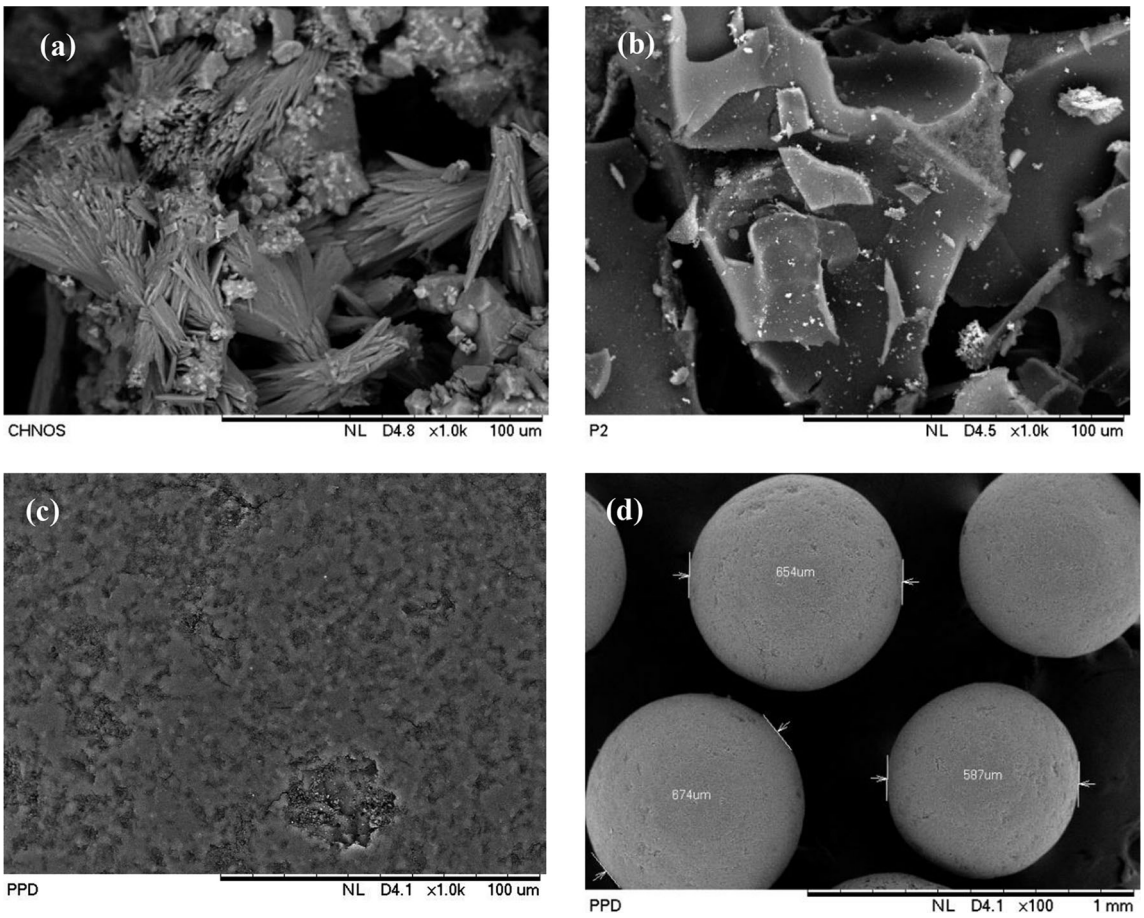

Fig. 1 SEM images of **a** R0; **b** R2; **c** PPD at × 1000 magnification; **d** PPD at × 100 magnification

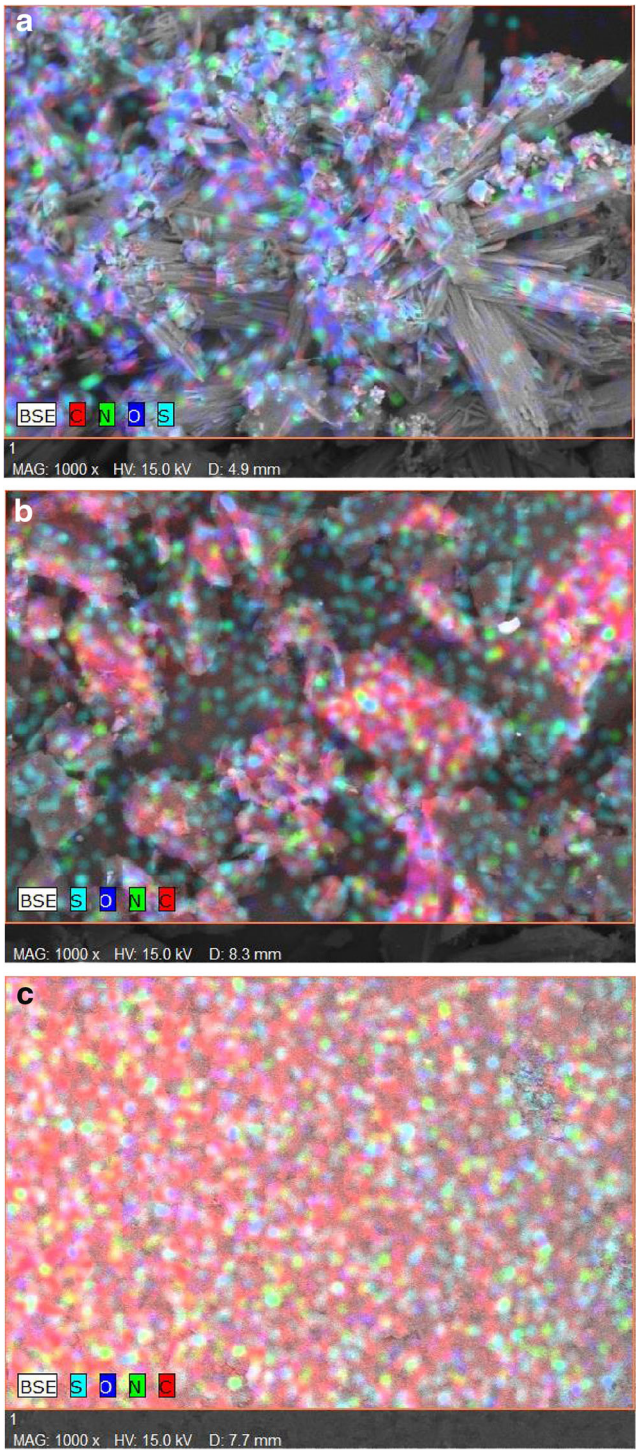

Fig. 2 EDX images of **a** R0, **b** R2, and **c** PPD

oxygen-rich surface of 74.1% due to uncontrolled pyrolysis. R2 has a 70.1% carbon content, which is three times greater than R0. PPD exhibits a high carbon content of 83.2%. The distribution of carbon element in R2 is comparable with that of PPD.

Figure S4 shows the pH_{PZC} plots for R0, R2.5, and PPD, and the respective values were determined as 3.6, 3.6, and 7.7, respectively (Table 4). The solution pH that is lesser than pH_{PZC} renders a positively charged carbon surface. Conversely, the carbon surface is surrounded by OH^- ions at solution pH higher than pH_{PZC} for a negatively charged surface. At pH > pH_{PZC}, the activated carbon is anionic, counteracts strong bases, and provides a high affinity towards cationic dye [19].

The surface functional groups of some activated carbons were quantitatively determined by Boehm titration. Table 4 displays the concentrations of acidic and basic groups in R2, R2.5, and PPD. The basic functional groups are usually oxygen-containing species like chromenes, ketones, pyrones, carbonyls, ethers, and π-electron system of carbon basal planes, while carboxyls, lactones, and phenols are the acidic functional group [20]. The GPD-derived activated carbons are relatively rich in total acidic functional groups (1.95–2.40 mmol/g) with a low density of basic groups (0.357–1.07 mmol/g). The functional groups are essential for interactions between the carbon surface and dye molecules in aqueous solution.

The nature of GPD and $ZnCl_2$ impregnation greatly affect the density of surface groups. The reaction between oxygen groups in GPD and $ZnCl_2$ modifies the chemical properties of activated carbon, converting it into material rich in oxygen-containing acidic groups with anionic character. From Table 4, the increase of impregnation ratio from 2 to 2.5 increases the concentration of acidic groups. The concentration of carboxylic groups notably increased nearly 4 times from 0.45 to 1.95 mmol/g. The surface deprotonation would take place at pH > pH_{PZC} due to the dissociation of acidic functional groups, hence decreasing the surface acidity of activated carbon. At this point, the increase in solubility allows the cationic dye molecules to coordinate to take up the position of H^+.

During the activation process, neutralization reaction would take place between $ZnCl_2$ (Lewis acid) and existing acidic moieties in GPD. For example, zinc phenolate and hydrogen chloride are produced from the neutralization of phenol hydroxyl (an organic weak acid) with $ZnCl_2$ [21]. As a result, the concentration of surface phenolic groups is almost negligible in GPD activated carbons.

Figure 3 shows the spectra of GPD and activated carbons. In Fig. 3a, the broad absorption band at 3370 cm^{-1} is generally assigned to OH hydrogen-bonded stretching vibration of alcohol and phenols, and NH stretching vibration of amines. The absorption band between 2930 and 2880 cm^{-1} shows the stretching vibrations of alkanes. The peak at 1590 cm^{-1} is the characteristic of NH_2 bending vibration of amines. The peak around 1420 cm^{-1} corresponds to α-CH_2 bending vibration of aldehydes and ketones. The absorption band between 1110 and 1040 cm^{-1} shows the C-N stretching vibration of amines, while the band at 930 cm^{-1} is associated with the bending vibrations of =CH, $=CH_2$ in alkenes. The peak at

Table 4 Surface functional groups of activated carbons

Activated carbon	pH_{PZC}	pH	Surface functional groups (mmol/g)				
			Carboxylic	Lactonic	Phenolic	Total acidic	Basic
R2	3.6	3.2	0.45	1.5	3.3×10^{-16}	1.95	1.07
R2.5	3.6	3.4	1.95	0.45	6.7×10^{-16}	2.4	0.357
PPD	7.7	5.3	0.6	0.15	0.45	1.2	1.43

860 cm^{-1} affirms the out-of-plane bending vibration of alkenes. The absorption band around 680 cm^{-1} indicates the bending vibration of cis-RCH═CHR alkenes.

Figure 3b displays the functional groups of activated carbons. After chemical treatment with $ZnCl_2$, the FTIR spectrum of R2 becomes more simplified. It signifies that most volatile matters and functional groups are released during pyrolysis. Most peaks in the range of 1650 to 460 cm^{-1} in GPD are disappeared, while some are diminished in intensity upon chemical activation. Generally, the FTIR spectra of R2 and PPD are identical, suggesting similar surface chemistry in both activated carbons. The peak at 2370 cm^{-1} is attributed to the conjugated C═C π-system, while the absorption band at 1530 cm^{-1} signifies the C═C aromatic ring stretching vibration. These frequencies generally represent a graphitic structure of activated carbon.

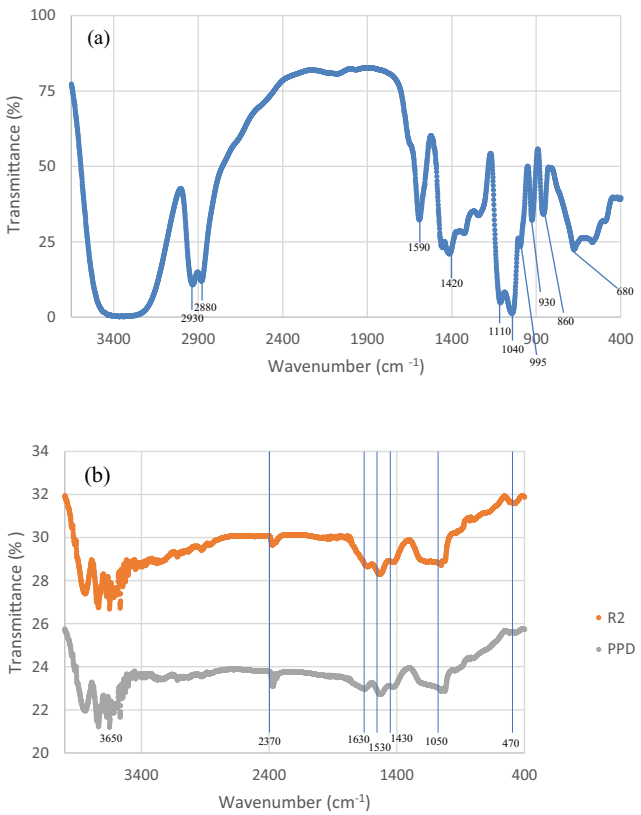

Fig. 3 FTIR spectra of **a** GPD and **b** R2 and PPD

3.2 Equilibrium adsorption

Figure 4 displays the equilibrium adsorption of methylene blue by GPD activated carbons and PPD. Generally, the adsorption capacity increased with increasing dye concentration to a saturation point, which is also known as maximum adsorption capacity. Adsorption is concentration-dependent at low concentration, in which the amount of dye molecules for adsorption sites becomes a limiting factor. As concentration increases approaching surface saturation, the number of active sites is quickly occupied and becomes a limiting factor. Moreover, the gradient provides a driving force for dye molecules to overcome mass transfer resistance at the solid phase.

R2 and R2.5 display the highest maximum adsorption capacity of 368 and 342 mg/g, respectively. R2 also exhibits a greater capacity of methylene blue than some methylene blue adsorbents from literature: palm fatty acid distillate char (7.6 mg/g) [13], pineapple waste–based activated carbon (288 mg/g) [22], *Pongamia pinnata* hull–based activated carbon (239 mg/g) [23], coated palygorskite activated carbon (351 mg/g) [24], and fishery waste–based activated carbon (184 mg/g) [25]. R2 and R2.5 also demonstrate a comparable removal performance with PPD (383 mg/g) due to their mesopore-rich content. R0 (50.4 m^2/g) displays a poor adsorption capacity because of the underdeveloped pore volume when compared with R2 (377 m^2/g) and R2.5 (267 m^2/g).

Table 5 summarizes the isotherm constants for methylene blue adsorption by activated carbons.

The Redlich-Peterson model is a three-parameter empirical equation that integrates the features of Langmuir and Freundlich models. The constants were computed through non-linear regression using Solver of MS Excel. The $g < 1$ often reflects the restriction of large molecules to form monolayer coverage due to solid impediment in active pores. From Table 5, the values of g are ranging from 0.854 to 1. When $g = 1$, the equation becomes Langmuir isotherm, which indicates an ideal monolayer adsorption onto a homogeneous surface. The equation is simplified to Henry's law, a form Freundlich isotherm when $1/K_R$ is equal to zero when $g = 0$. In this work, K_R and a_R were found to be in the range of 12.0 to 137 and 0.0295 to 1.61, respectively. The equilibrium data obeyed Langmuir and Redlich-Peterson models with $R^2 > 0.910$, suggesting the predominance of monolayer coverage of dye molecules on the carbon surface.

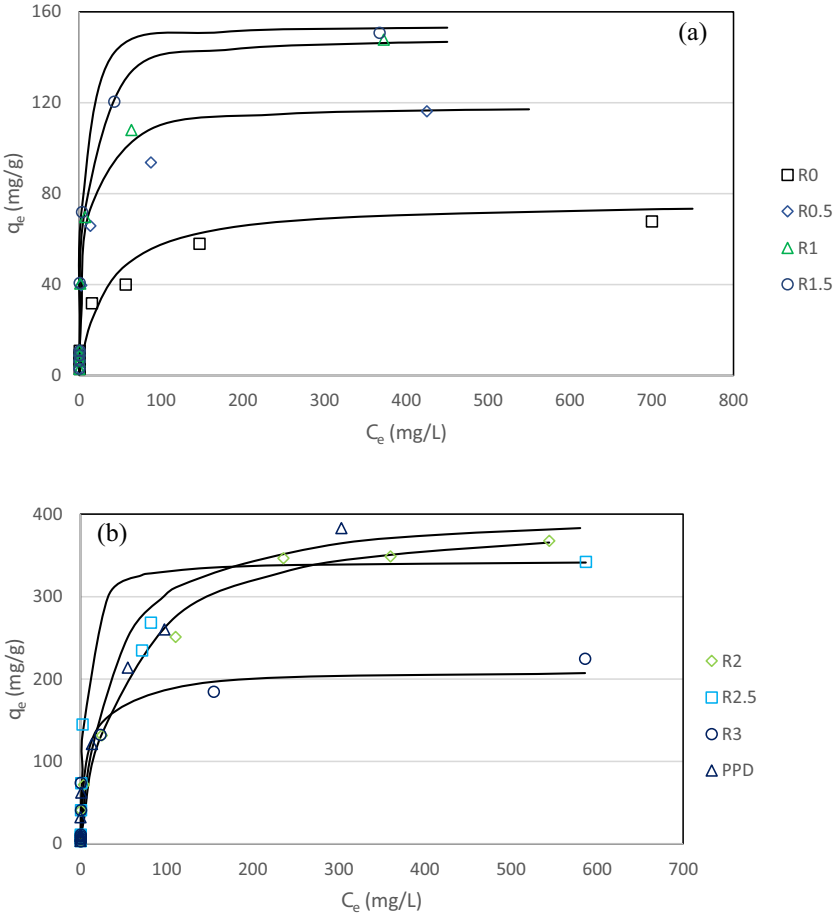

Fig. 4 Equilibrium adsorption of methylene blue onto activated carbons. **a** R0, R0.5, R1, and R1.5. **b** R2, R2.5, R3, and PPD (Lines were predicted by Langmuir model)

The Langmuir constant, b, is an important parameter that signifies the adsorption affinity at low concentration. The adsorption capacity tends to move towards the ordinate indicating a favorable process at low concentration. The high affinity may not necessarily imply high adsorption capacity as concentration increases in the direction of equilibrium.

The Freundlich isotherm is the least satisfactory model to describe the adsorption data. Hence, the adsorption mechanism may not due to multilayer formation over a heterogeneous surface. The Dubinin-Radushkevich model was used to determine the porosity and apparent adsorption capacity. The equation somewhat underpredicts the Q_s values when

Table 5 Isotherm constants for methylene blue adsorption by activated carbons

Activated carbon	Q_{exp} (mg/g)	Langmuir			Freundlich			Redlich-Peterson				Dubinin-Radushkevich		
		Q_m (mg/g)	b (L/mg)	R^2	n	K (mg/g) (L/mg)$^{1/n}$	R^2	g	K_R (L/g)	a_R (L/mg)^g	R^2	Q_s (mg/g)	E (kJ/mol)	R^2
R0	68	76.6	0.0304	0.947	3.80	14.5	0.924	0.924	33.6	1.61	0.924	63.9	8.22	0.879
R0.5	116	119	0.118	0.966	3.81	27.4	0.949	0.855	42.3	0.855	0.978	114	6.07	0.924
R1	151	149	0.135	0.952	3.46	30.9	0.933	0.854	47.5	0.701	0.968	141	3.68	0.921
R1.5	151	154	0.273	0.965	3.77	37.5	0.907	0.907	61.0	0.611	0.974	163	13.5	0.888
R2	368	399	0.0203	0.988	2.96	47.9	0.982	0.982	22.8	0.204	0.988	336	14.4	0.958
R2.5	342	344	0.262	0.912	3.75	80.6	0.897	0.897	137	0.736	0.910	331	1.41	0.900
R3	224	210	0.0963	0.922	4.08	47.5	0.901	0.864	128	1.40	0.938	180	0.656	0.849
PPD	383	406	0.0295	0.939	3.91	83.1	0.916	1.00	12.0	0.0295	0.916	306	0.834	0.790

compared with Q_{exp}. Also, E is the mean free energy of adsorption: $E < 8$ kJ/mol is a characteristic of physical adsorption, while 8 kJ/mol < E < 16 kJ/mol indicates an electrostatic interaction, and $E > 16$ kJ/mol is an attribute of chemical adsorption [26]. From Table 5, the range of E suggests the interplay of physisorption and electrostatic interaction as the driven mechanisms for methylene blue adsorption by GPD activated carbons. The adsorption process could be instigated through van der Waals force, mesopore filling, electrostatic attraction, π-π stacking between aromatic rings of dye molecule and carbon graphitic layer, and complex formation with surface functional groups. Conversely, the primary mechanism for PPD is physical adsorption.

In Langmuir isotherm, the separation factor, R_L, is a dimensionless constant to explain the nature of adsorption [27]. It is given as:

$$R_L = \frac{1}{1 + bC_o} \tag{3}$$

The adsorption is unfavorable when $R_L > 1$, non-linear when $R_L = 1$, favorable when $0 < R_L < 1$, or irreversible at $R_L = 1$. Figure S5 shows the R_L profiles for methylene blue adsorption by activated carbons. The R_L values are in the range of 0 to 1, indicating a favorable adsorption process at the experimental conditions.

3.3 Adsorption kinetics

The effect of contact time on the adsorption of methylene blue was determined at different concentrations, and the results are shown in Fig. 5. Generally, the rate of adsorption decreased with increasing contact time to a point of equilibrium. GPD activated carbons showed a greater removal capacity than PPD at C_o = 20 mg/L. The time taken for GPD activated carbons to reach equilibrium is around 3 days, as opposed to 7 days by PPD. Moreover, the adsorption capacity at equilibrium by all GPD activated carbons at this concentration is comparable at 11.7 mg/g.

The adsorption is rapid at the beginning of solid contact in solution because of plentiful active sites for adsorption. The external diffusion is normally fast, while the diffusion into internal pores is a slower process. As time progresses, the adsorption capacity begins to be leveling off. At this stage,

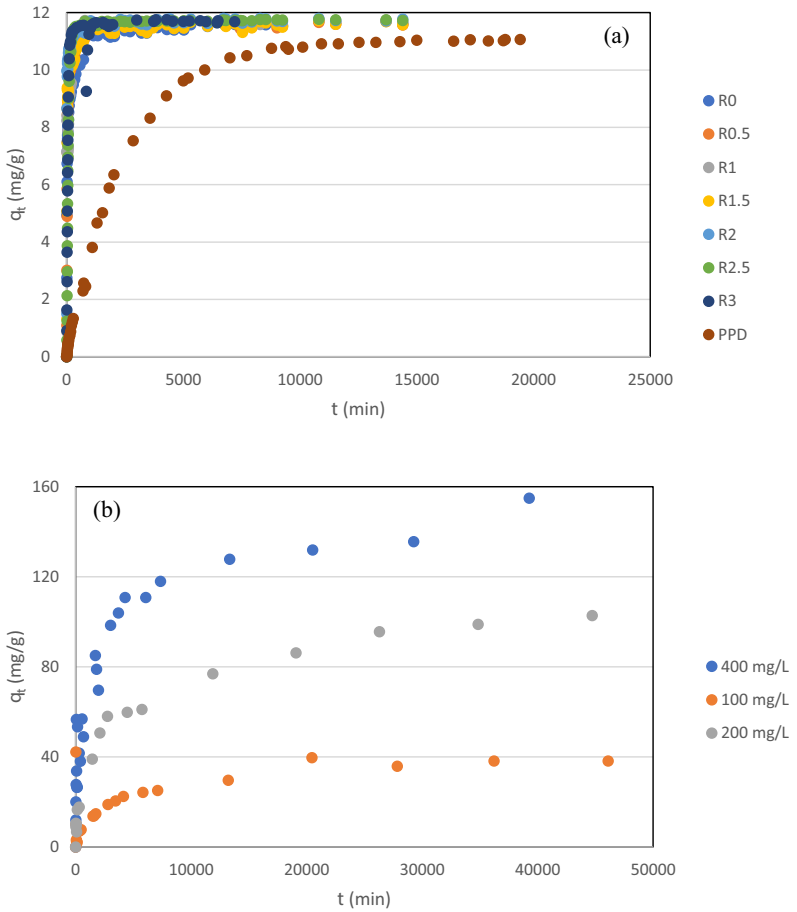

Fig. 5 Effect of contact time on equilibrium adsorption of methylene blue by **a** all activated carbons at C_o = 20 mg/L; **b** R2.5 at C_o = 100, 200, and 400 mg/L

the readily adsorbed dye may display the same charge that triggers repulsion with free molecules in bulk solution, making the slowly occupied sites remain vacant. The desorption of dye from the surface could also occur because of weak bond energy. Consequently, the equilibrium is achieved.

The increase in concentration increases the adsorption rate and time taken to attain equilibrium. A high concentration offers greater driving force for dye molecules to surpass mass transfer resistance for a high adsorption rate. However, the available sites are crowded with the approaching molecules, thus delaying the equilibrium time. Conversely, the sites are readily accessible at low concentration for rapid equilibrium although the initial adsorption rate is low.

The kinetics study is necessary to explain the uptake rate and controlling steps in the adsorption process. Table 6 summarizes the kinetic constants of methylene blue adsorption by activated carbons. Generally, the pseudo-second-order equation shows a better fitting to kinetics data with a close agreement between calculated q_e and experimental q_e as compared with pseudo-first-order equation, particularly at high concentration. The pseudo-first-order equation did not obey the kinetics data for the entire range of contact time at high concentration. A high dye concentration induces stronger molecular repulsion and competition for active sites, thus restricting the external diffusion as a significant adsorption step. Consequently, the rate constant and adsorption rate decreased with concentration, resulting in a longer contact time to reach equilibrium. This further suggests that the adsorption at high concentration proceeds via chemical-type interaction between oxygen-containing functional groups in carbon surface and cationic dye molecules. Chemical adsorption (chemisorption) is irreversible because of strong bonding and site-specific, where the chemically adsorbed molecules are lodged to certain sites, forming a one molecule thick layer of adsorbed species.

The rate constant of intraparticle diffusion, k_{diff}, was determined from the gradient of q_t versus $t^{0.5}$, while C is the intercept by extrapolating the linear section to the ordinate. The C value is proportional to the extent of the boundary layer thickness [26]. If the straight line of q_t versus $t^{0.5}$ passes through the origin ($C = 0$), then intraparticle diffusion is the sole rate-limiting step, where the boundary layer diffusion (film diffusion) is insignificant. As the straight lines deviate from the origin ($C > 0$), the intraparticle diffusion is not the only rate-controlling step. Moreover, the positive C signifies a certain controlling degree of film diffusion and rapid adsorption.

Table 6 Kinetic parameters for methylene blue adsorption onto GPD activated carbons

Activated carbon	C_o (mg/L)	q_{exp} (mg/g)	Pseudo-first-order			Pseudo-second-order			Intraparticle diffusion			Boyd's		
			q_{cal} (mg/g)	k_1 (min^{-1})	R^2	q_{cal} (mg/g)	k_2 (g/mg/h)	R^2	k_{diff}	C	R^2	B	D_i (cm^2/s)	R^2
R0	5	0.486	0.468	0.00596	0.747	0.496	0.0133	0.661	0.00748	0.119	0.524	2×10^{-4}	4.85×10^{-10}	0.843
R0.5		3.78	3.65	0.0133	0.851	3.76	0.00586	0.882	0.025	1.97	0.644	5×10^{-5}	1×10^{-10}	0.942
R1		3.74	3.55	0.00268	0.829	3.86	0.000829	0.811	0.0394	0.677	0.615	2×10^{-5}	4.85×10^{-10}	0.766
R1.5		3.85	3.63	0.00215	0.864	4.01	0.000604	0.844	0.0455	0.289	0.640	1×10^{-5}	2.42×10^{-11}	0.549
R2		3.89	3.66	0.0422	0.680	3.74	0.0234	0.822	0.0169	2.65	0.525	5×10^{-5}	7×10^{-11}	0.805
R2.5		3.88	3.56	0.0354	0.582	3.63	0.02	0.728	0.0189	2.45	0.613	1×10^{-5}	2×10^{-11}	0.724
R3		3.76	3.34	0.0204	0.558	3.43	0.0110	0.657	0.0225	1.98	0.719	1×10^{-5}	2.42×10^{-11}	0.769
PPD		3.46	3.40	0.00056	0.993	3.78	0.0002	0.993	0.0273	0.411	0.915	6×10^{-6}	1.5×10^{-11}	0.985
R0	10	5.91	5.52	0.012	0.928	5.64	0.0034	0.951	0.0207	3.59	0.538	5×10^{-6}	1.2×10^{-11}	0.488
R0.5		5.90	5.74	0.084	0.892	5.81	0.0274	0.955	0.0081	5.04	0.246	1×10^{-5}	2.40×10^{-11}	0.683
R1		5.80	5.59	0.0498	0.804	5.64	0.0172	0.897	0.012	4.52	0.350	2×10^{-5}	5×10^{-11}	0.687
R1.5		5.80	5.51	0.107	0.686	5.61	0.0288	0.854	0.01107	4.67	0.377	3×10^{-5}	7.27×10^{-11}	0.576
R2		5.83	5.57	0.0265	0.692	5.65	0.00919	0.801	0.0169	4.14	0.530	6×10^{-6}	1.45×10^{-11}	0.682
R2.5		5.90	5.79	0.0384	0.989	5.86	0.0121	0.983	0.0130	4.63	0.299	4×10^{-6}	9.70×10^{-12}	0.675
R3		5.90	5.76	0.0202	0.987	5.86	0.00556	0.978	0.0189	4.04	0.386	5×10^{-6}	1.21×10^{-11}	0.611
PPD		6.45	6.27	0.000581	0.988	6.96	0.000114	0.987	0.0500	0.813	0.907	5×10^{-6}	1.21×10^{-11}	0.935
R0	15	10.2	9.25	0.0280	0.787	9.57	0.00478	0.842	0.0694	5.84	0.563	5×10^{-5}	1.21×10^{-10}	0.789
R0.5		10.4	9.85	0.0572	0.862	10.2	0.00967	0.942	0.0361	7.66	0.370	1×10^{-5}	2.42×10^{-11}	0.645
R1		10.3	9.52	0.0485	0.768	9.83	0.00849	0.896	0.0409	7.08	0.475	9×10^{-6}	2.18×10^{-11}	0.636
R1.5		10.3	9.58	0.0805	0.701	9.97	0.0117	0.877	0.0360	7.60	0.434	2×10^{-5}	4.85×10^{-11}	0.800
R2		10.3	9.78	0.0917	0.809	10.1	0.0143	0.918	0.0311	8.02	0.335	2×10^{-5}	4.85×10^{-11}	0.819
R2.5		10.3	10.1	0.0961	0.963	10.3	0.0180	0.975	0.0236	8.63	0.210	2×10^{-5}	4.85×10^{-11}	0.687
R3		10.3	10.1	0.0368	0.979	10.4	0.00610	0.946	0.0397	7.40	0.311	1×10^{-5}	2.42×10^{-11}	0.715
PPD		8.95	8.63	0.0004	0.988	10.0	0.0000483	0.990	0.0704	0.695	0.948	4×10^{-6}	9.7×10^{-12}	0.965
R0	20	11.7	11.0	0.0317	0.848	11.3	0.00474	0.948	0.0486	7.76	0.534	7×10^{-7}	1.70×10^{-12}	0.729
R0.5		11.7	11.3	0.0333	0.950	11.6	0.00482	0.979	0.0442	8.22	0.387	1×10^{-5}	2.42×10^{-11}	0.703
R1		11.8	11.2	0.0330	0.751	11.4	0.00524	0.868	0.0461	8.09	0.453	8×10^{-6}	1.94×10^{-11}	0.510
R1.5		11.7	11.1	0.0525	0.888	11.4	0.00788	0.947	0.0370	8.72	0.356	1×10^{-5}	2.42×10^{-11}	0.669
R2		11.8	11.4	0.0901	0.793	11.7	0.0137	0.911	0.0266	9.70	0.222	5×10^{-5}	1.21×10^{-10}	0.628
R2.5		11.8	11.7	0.0150	0.994	12.1	0.00187	0.970	0.0633	6.93	0.415	5×10^{-5}	1.21×10^{-10}	0.656
R3		11.7	11.5	0.0206	0.983	11.9	0.00268	0.961	0.0828	6.95	0.426	3×10^{-5}	7.27×10^{-11}	0.671
PPD		11.1	11.1	0.000401	0.999	12.9	0.0000353	0.994	0.0950	0.347	0.921	6×10^{-3}	1.45×10^{-8}	0.747

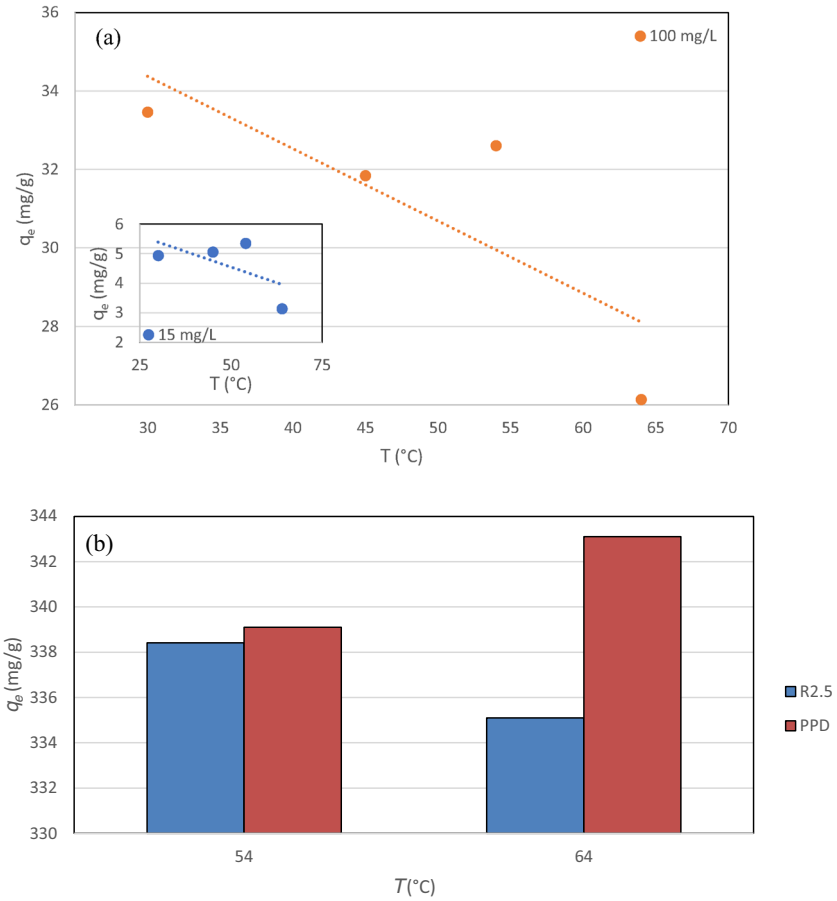

Fig. 6 **a** Effect of temperature on methylene blue removal by R2 at C_o = 15 mg/L (inset) and 100 mg/L. **b** Effect of temperature on methylene blue removal by R2.5 and PPD at C_o = 1000 mg/L

Adsorption process normally consists of four sequential steps: (i) migration of dye from the bulk of solution to the surface of adsorbent (bulk diffusion), (ii) diffusion of dye through the boundary layer to the surface of adsorbent (film diffusion), (iii) intraparticle diffusion of dye into the interior pores of adsorbent, and (iv) adsorption of dye at the active sites (surface diffusion). Adsorption of molecules inside the pores is generally a fast step; hence, it could not be regarded as a rate-controlling step. Thus, the adsorption process is either governed (controlled) by particle diffusion or film diffusion. This can be predicted by Boyd's equation via the linearity of B_t versus t. The Boyd's lines for all activated carbons are not

Table 7 Thermodynamic parameters for methylene blue adsorption by activated carbons

C_o (mg/L)	$\Delta G°$ (kJ/mol)				$\Delta H°$ (kJ/mol)	$\Delta S°$ (J/mol/K)
	30 °C	45 °C	54 °C	64 °C		
R2						
15	− 10.5	− 5.98	− 12.1	− 0.981	− 69.4	− 0.193
100	− 14.3	− 11.9	− 14.1	− 15.8	− 0.138	0.044
400	− 2.46	− 4.66	− 4.78	− 19.5	129	0.425
R2.5						
15	− 18.7	− 9.58	− 11.3	− 10.8	− 86.2	− 0.229
100	− 19.3	− 11.0	− 14.4	− 18.3	− 29.9	− 0.044
400	− 5.34	− 9.50	− 6.97	− 20.3	104	0.357
PPD						
15	− 12.4	− 13.1	− 10.8	− 10.0	− 35.9	− 75.6
100	− 13.6	− 19.0	− 17.8	− 16.1	10.0	0.00828
400	− 3.32	− 12.0	− 18.3	− 21.1	161	0.545

linear and did not pass through the origin, suggesting that the intraparticle diffusion is not the dominant rate-controlling step. From Table 6, the effective diffusion coefficient, D_i, is in the range of 10^{-12} to 10^{-8} cm^2/s, implying a cooperative mechanism of particle diffusion and film diffusion that controls the adsorption process.

3.4 Adsorption thermodynamics

Figure 6 shows the effect of temperature in dye adsorption by selected GPD activated carbons and PPD, and the thermodynamic parameters are summarized in Table 7. The activated carbons demonstrate a similar pattern of $\Delta H°$ shifting from exothermic at low concentration to endothermic at high concentration. Generally, the viscosity of the solution decreases when the surrounding (solution) temperature is high, which aids the mobility of molecules to diffuse from the external layer into internal pores of activated carbon. The adsorption of methylene blue at high concentration is endothermic in nature because the removal capacity increases with increasing temperature. At C_o = 1000 mg/L, R2.5 displays a similar performance with PPD at temperatures of 54 °C and 64 °C. A comparable capacity was recorded at about 334 mg/g.

Additionally, the magnitude of $\Delta G°$ becomes more negative with increasing temperature, suggesting that the adsorption of methylene blue is thermodynamically feasible, favorable, and spontaneous. Accordingly, $\Delta S°$ is positive, showing the inconsistent increase in orientation disorder and randomness of molecules arrangement at carbon-solution interface during adsorption. Both $\Delta H°$ and $\Delta S°$ increased when the dye solution becomes more concentrated, signifying an endothermic process with increasing randomness. At high concentration, dye molecules are tightly packed with each other, restricting the movement, consequently escalating the degree of disorder. Similarly, the frequent collision among molecules and carbon walls induces more kinetics energy, decreasing the energy within the system, thus demanding for extra external heat [26].

4 Conclusion

Glycerine pitch distillate was successfully converted into activated carbons by chemical activation using $ZnCl_2$. The surface area of activated carbons is $ZnCl_2$ ratio-dependent, which is in the range of 50.4–804 m^2/g. The GPD activation at ratio 2 (R2, 377 m^2/g) exhibits a 368-mg/g methylene blue capacity that is comparable with the performance of commercial activated carbon (PPD, 1187 m^2/g). The mesoporous nature of R2 improves the diffusion path for dye molecules despite its low surface area than that of PPD. The thermodynamic parameters conclude that the adsorption of methylene blue is endothermic and spontaneous. The activated carbons exhibit favorable adsorption properties for potential applications in dye wastewater treatment.

Acknowledgments The authors thank Prof. Dr. Motoi Machida and Dr. Yoshimasa Amano of Chiba University, Japan, for the gift of commercial petroleum pitch distillate-based activated carbon.

Funding information This study is financially supported by the UTM Research University Grant No. 07G80.

Compliance with ethical standards

Conflict of Interest The authors declare that they have no conflict of interest.

References

1. Ming-Twang S, Lin-Zhi L, Zaini MAA, Zhi-Yong Q, Pei-Yee AY (2015) Activated carbon for dyes adsorption in aqueous solution. Adv Environ Res *36*:217–234
2. García JR, Sedran U, Zaini MAA, Zakaria ZA (2018) Preparation, characterization, and dye removal study of activated carbon prepared from palm kernel shell. Environ Sci Pollut Res 26(5):5076–5085
3. Sakamoto T, Zaini MAA, Amano Y, Machida M (2019) Preparation and characterization of activated carbons produced from oil palm empty fruit bunches. TANSO 286:9–13
4. Yan KZ, Zaini MAA, Arsad A, Nasri NS (2019) Rubber seed shell based activated carbon by physical activation for phenol removal. Chem Eng Trans 72:151–156
5. Hock PE, Zaini MAA (2018) Activated carbons by zinc chloride activation for dye removal - a commentary. Acta Chim Slov 11(2):99–106
6. Zaini MAA, Meng TW, Kamaruddin MJ, Setapar SHM, Yunus MAC (2014) Microwave-induced zinc chloride activated palm kernel shell for dye removal. Sains Malaysiana 43(9):1421–1428
7. Spagnoli AA, Giannakoudakis DA, Bashkova S (2016) Adsorption of methylene blue on cashew nut shell based carbons activated with zinc chloride: the role of surface and structural parameters. J Mol Liq 229:465–471. https://doi.org/10.1016/j.molliq.2016.12.106
8. Yong KC, Ooi TL, Dzulkefly K, Wan-Yunus WMZ, Hazimah AH (2001) Refining of crude glycerine recovered from glycerol residue by simple vacuum distillation. J Oil Palm Res 13(2):39–44
9. Merapan K (2015). Glycerine pitch from glycerine concentration process as alternative fuel for boiler operation. Master Dissertation, Universiti Teknologi Malaysia
10. Foo KY, Hameed BH (2009) Utilization of biodiesel waste as a renewable resource for activated carbon: application to environmental problems. Renew Sust Energ Rev 13:2495–2504
11. Aderemi HB, Zaini MAA, Nasri NS (2018) Adsorbents from the by-product of palm oil refinery for methylene blue removal. Malaysian J Anal Sci 22(4):642–647
12. Swan NB, Zaini MAA (2019) Adsorption of malachite green and Congo red dyes from water: recent progress and future outlook. Ecol Chem Eng S 26(1):119–132
13. Aderemi HB, Nasri NS, Zaini MAA (2018) Physicochemical properties of char derived from palm fatty acid distillate. Malaysian J Fundament Appl Sci 14(3):403–406
14. Kumar R, Chandrashekar N (2014) Fuel properties and combustion characteristics of some promising bamboo species in India. J For Res 25(2):471–476

15. Angın D (2013) Production and characterization of activated carbon from sour cherry stones by zinc chloride. Fuel 115:804–811
16. Tang SH, Zaini MAA (2015) Potassium hydroxide activation of activated carbon: a commentary. Carbon Lett 16(4):275–280
17. Sing et al (1985) Reporting physisorption data for gas/solid systems with special reference to the determination of surface area and porosity. Pure Appl Chem 57:603–619
18. Sulaiman NS, Zaini MAA, Arsad A (2020) Evaluation of dyes removal by beta-cyclodextrin adsorbent. Mater Today Proc. https://doi.org/10.1016/j.matpr.2020.03.696
19. Bernal V, Erto A, Giraldo L, Moreno-Piranjan JC (2017) Effect of solution pH on the adsorption of paracetamol on chemically modified activated carbons. Molecules 22(7):1032. https://doi.org/10.3390/molecules22071032
20. Boehm HP (2002) Surface oxides on carbon and their analysis: a critical assessment. Carbon 40:145–149
21. Wongsiriwan U, Noda Y, Song CS, Prasassarakich P, Yeboah Y (2010) Lignocellulosic biomass conversion by sequential combination of organic acid and base treatments. Energy Fuel 24:3232–3238
22. Mahamad MN, Zaini MAA, Zakaria ZA (2015) Preparation and characterization of activated carbon from pineapple waste biomass for dye removal. Int Biodeterior Biodegrad 102:274–280. https://doi.org/10.1016/j.ibiod.2015.03.009
23. Islam MA, Sabar S, Benhouria A, Khanday WA, Asif M, Hameed BH (2017) Nanoporous activated carbon prepared from karanj (Pongamia pinnata) fruit hulls for methylene blue adsorption. J Taiwan Inst Chem Eng 74:96–104. https://doi.org/10.1016/j.jtice.2017.01.016
24. Zhang XL, Cheng LP, Wu XP, Tang YZ, Wu YC (2015) Activated carbon coated palygorskite as adsorbent by activation and its adsorption for methylene blue. J Environ Sci 33:97–105. https://doi.org/10.1016/j.jes.2015.01.014
25. Marrakchi F, Auta M, Khanday WA, Hameed BH (2017) High-surface-area and nitrogen-rich mesoporous carbon material from fishery waste for effective adsorption of methylene blue. Powder Technol 321:428–434. https://doi.org/10.1016/j.powtec.2017.08.023
26. Lee LZ, Zaini MAA (2017) Adsorption properties of cationic rhodamine B dye onto metals chloride-activated castor bean residue carbons. Water Sci Technol 75(4):864–880
27. Webber TW, Chakkravorti RK (1974) Pore and solid diffusion models for fixed-bed adsorbers. AlChE J 20:228–238

Publisher's Note Springer Nature remains neutral with regard to jurisdictional claims in published maps and institutional affiliations.